Design of an ultra-low power device for aircraft structural health monitoring

Alessandro Perelli*, Carlo Caione*, Luca De Marchi*, Davide Brunelli†, Alessandro Marzani‡ and Luca Benini*

*Department of Electrical, Electronic and Information Engineering - DEI, University of Bologna, Italy.
† Department of Industrial Engineering - DII, University of Trento, Italy.
‡Department of Civil, Chemical, Environmental and Materials Engineering - DICAM, University of Bologna, Italy.

Abstract—One of the popular structural health monitoring (SHM) applications of both automotive and aeronautic fields is devoted to the non-destructive localization of impacts in plate-like structures. The aim of this paper is to develop a miniaturized, self-contained and low power device for automated impact detection that can be used in a distributed fashion without central coordination. The proposed device uses an array of four piezoelectric transducers, bonded to the plate, capable to detect the guided waves generated by an impact, to a STM32F4 board equipped with an ARM Cortex-M4 microcontroller and a IEEE802.15.4 wireless transceiver. The waves processing and the localization algorithm are implemented on-board and optimized for speed and power consumption. In particular, the localization of the impact point is obtained by cross-correlating the signals related to the same event acquired by the different sensors in the warped frequency domain. Finally the performance of the whole system is analysed in terms of localization accuracy and power consumption, showing the effectiveness of the proposed implementation.

I. Introduction

Damages to aircraft and high-speed vehicles caused by the impact of debris and flying objects is a critical concern for automotive and aeronautic systems. Such damages, in fact, if not detected and repaired at an early stage might grow leading to the failure of the systems. In this context, Structural health monitoring (SHM) technologies, by embedding smart sensors into the structures and responding/adapting to changes in condition, can allow for an automatic detection of defects due to impacts. Among the number of SHM approaches, the one based on guided waves (GW) is considered as the most promising and versatile. In fact, an impact at high speed produces detectable acoustic and ultrasonic guided waves on the structural component. These waves can be used to compute the location of the impact and eventually to assess the damage. In general, GW based technologies for SHM exploit a network of piezoelectric transducers positioned on the structure to inspect. The minimization of the array elements is fundamental to reduce not only the hardware complexity associated with transducer wiring and multiplexing circuitry but also the intensive signal processing of the large amounts of recorded data. For this reason, there is growing interest in minimizing the number of sensors by optimizing their positioning, as well as by increasing the resolution of impact localization procedures [1]. Another current trend in the SHM field is to create wireless sensor networks with low power consumption or even energetically autonomous [2], [3]. One promising solution would be a SHM system that could be embedded into the structure, inspect the structural hot spots and download data or diagnostic results wirelessly to a remote station [4], [5], [6]. A lot of literature has been produced on the use of sensor-array-based methods for high-speed acquisition and data processing. However, generally such approaches use a large number of individual sensors that usually are bulky, heavy and require wiring back to a central location. Moreover when large-scale deployment are implied, the power consumption of the system is hardly sustainable by the ordinary generation system present on board. In contrast to these traditional transducers, wireless sensors technology integrating small sensors and wireless communication are becoming vital in SHM, guaranteeing at the same time: (1) less wiring among sensors and between sensors and the central unit; (2) lower weight; (3) reduced power consumption and (4) real-time monitoring even in harsh environmental conditions.

In this paper we propose a new PZT-based wireless embedded ultrasonic structural monitoring system for impact localization with advantages over traditional systems of compactness, light weight, low-power consumption and high efficiency and precision. The passive approach based on ultrasonic Lamb waves and conventional piezoelectric transducers (PZT discs) is capable of achieving high localization performance using a dispersion compensation algorithm with low computational cost. The structure of the SHM system is illustrated in Fig. 1. In the new SHM system, the signal conditioning, amplification and A/D converting circuits are replaced by a simple comparator circuit, in which the response signal from a piezoelectric transducer PZT sensor is directly changed into a digital queue by comparing it with a preset trigger value.
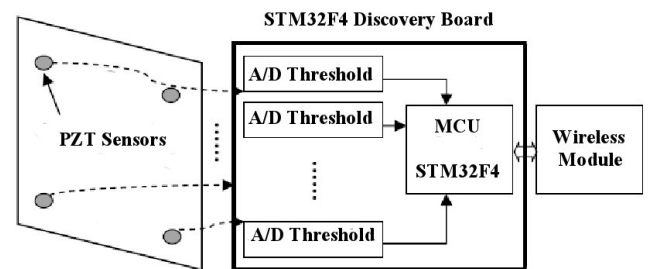

Fig. 1. Structure of the embedded SHM system for impact detection

The device samples the signals in passive mode using 4 different piezoelectric transducers and the signals are elaborated on a Cortex-M4 based microcontroller. By cross-correlating

the dispersion-compensated signals, the impact point can be determined via hyperbolic positioning. Thus, when an impact occurs, only the data of its position is recorded and sent to the central system through wireless transmission. The structure of this paper is as follows: in Section II the proposed compensation procedure based on the Warped Frequency Transform (WFT) is presented. The design and realization of the new PZT-based wireless digital impact monitoring system is described in detail in Section III. Section IV shows the feasibility and stability of the embedded ultrasonic structural monitoring system and an experimental validation is presented.

II. DISPERSION COMPENSATION USING THE WARPED FREQUENCY TRANSFORM

A. The warping frequency transform (WFT)

Given a dispersive guided wave signal $s(t)$ whose frequency representation is $S(f) = \mathbf{F}\{s(t)\}$, being $\mathbf{F}$ the Fourier Transform operator, the Frequency Warping operator $\mathbf{W}_w$ reshapes the periodic frequency axis by means of a proper function $w(f)$, called from now *warping map*, such as:

$$s_w(t) = \mathbf{W}_w\{s(t)\}, \quad \mathbf{F}\{s_w(t)\} = \sqrt{\dot{w}(f)} \cdot S(w(f))$$

where $s_w(t)$ is the warped signal, and $\dot{w}(f)$ represents the first derivative of $w(f)$. The Frequency Warping operator can be expressed as the composition of the Non-Uniform Fourier Transform (NUFFT) $\mathbf{F}_w$ and the classical Inverse Fourier Transform $\mathbf{F}^\dagger$:

$$\mathbf{W}_w = \mathbf{F}^\dagger \mathbf{F}_w \qquad (1)$$

It has been shown in [7], [8] that in order to compensate the signal with respect to a particular guided mode, $w(f)$ can be defined through its functional inverse, as:

$$K\frac{dw^{-1}(f)}{df} = \frac{1}{c_g(f)} \qquad (2)$$

where $\frac{1}{c_g(f)}$ is the nominal dispersive slowness relation of the wave to consider, being $c_g(f)$ its group velocity curve and K a normalization parameter selected so that $w^{-1}(0.5) = w(0.5) = 0.5$.
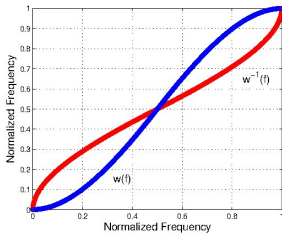

Fig. 2. Warping map $w(f)$ for A_0 wave dispersion compensation and its functional inverse $w^{-1}(f)$
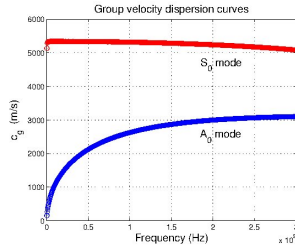
Fig. 3. $c_g(f)$ dispersion curves for the Lamb waves propagating in an aluminum 0.003 m thick-plate.

A sample warping map is depicted in Fig. 2 along with its functional inverse. It was computed according to Eq. (2) by considering the group velocity curve of the Lamb A_0 mode represented in Fig. 3. The curves in Fig.3 were obtained by using the Semi-Analytical Finite Element (SAFE) formulation proposed in [9] considering a 0.003 m thick aluminum plate

with Young modulus $E = 69$ GPa, Poisson's coefficient $\nu = 0.33$ and material density $\rho = 2700 \text{ kg} \cdot \text{m}^{-3}$.

The NUFFT is based on an oversampled Discrete Fourier Transform (DFT) followed by an interpolation method optimal in the min-max sense of minimizing the worst-case approximation error over all signals of unit norm [10]. To compute the DFT at a collection of (non uniformly spaced) frequency locations ω_m which represent the warping map $w(f)$, first a convenient $K \geq N$ must be assumed so that the K-point FFT of s_n $S(\omega_k) = \mathbf{F}\{s_n\} = \sum_{n=0}^{N-1} s_n e^{-j\frac{2\pi}{K}kn}$ $k = 1, \ldots, K$ where $\frac{2\pi}{K}$ is the fundamental frequency of the K-point DFT. The second step of most NUFFT methods is to approximate each $S(\omega_m)$ by interpolating $S(\omega)$ using some of the neighbors of ω_m in the DFT frequency set. Linear interpolators have the following general form:

$$\hat{S}(\omega_m) = \sum_{k=0}^{K-1} u_k^*(\omega_m) S(\omega_k) \quad m = 1, \ldots, M$$

where the $u_k^*(\omega_m)$ denote the interpolation coefficients selected through a min-max criterion. For each desired frequency location ω_m the coefficient vector the worst-case approximation error between $S(w(f))$ and $\hat{S}(\omega_m)$ is determined. As demonstrated in [10], the interpolator coefficients $u_k^*(\omega_m)$ can be obtained by an analytic formula derived from the following optimization criterion: $\min_{u(\omega_m) \in \mathcal{C}^J} \max_{s \in \mathcal{R}^N} |\hat{S}(\omega_m) - S(\omega_m)|$

B. Warping a wave detected passively

In passive monitoring techniques the time instant in which an acoustic emission starts is unknown. Let us consider the effect of warping when an actuated wave is excited at a generic instant t_{d_1}. The Fourier Transform of the actuated wave is given by: $S_a(f,0) = S_0(f,0) \cdot e^{-j2\pi t_{d_1} f}$ being $S_0(f,0)$ the Fourier Transform of the excited wave (incipient pulse centered in $t = 0$). An undamped guided wave at a traveled distance D from the source point, $s(t,D)$, can be modeled in the frequency domain as a dispersive system whose response is:

$$S(f,D) = S_0(f,0) \cdot e^{-j2\pi t_{d_1} f} \cdot e^{-j2\pi \int \tau(f,D)df} \qquad (3)$$

being $\tau(f,D)$ the group delay of the wave component of frequency f which can be assumed equal to:

$$\tau(f,D) = \frac{D}{c_g(f)} = D \cdot K \cdot \frac{dw^{-1}(f)}{df} \qquad (4)$$

In force of Eq. (3), (4) can be rewritten as:

$$S(f,D) = S_0(f,0) \cdot e^{-j2\pi t_{d_1} f} \cdot e^{-j2\pi w^{-1}(f)KD}$$

where the distortion results from the nonlinear phase term. Considering now that the generated dispersive wave $s(t,D_i)$ is acquired by two different sensors (1 and 2) after having travelled two different distances of propagation, D_1 and D_2. The Warped Fourier Transforms of the recorded signals $s(t,D_1)$ and $s(t,D_2)$ are given by:

$$\mathbf{FW}_w\{s(t,D_1)\} = \sqrt{\dot{w}(f)} \cdot S_0(w(f),0) \cdot e^{-j2\pi w(f) t_{d1}} \cdot e^{-j2\pi fKD_1}$$

$$\mathbf{FW}_w\{s(t,D_2)\} = \sqrt{\dot{w}(f)} \cdot S_0(w(f),0) \cdot e^{-j2\pi w(f) t_{d1}} \cdot e^{-j2\pi fKD_2}$$

where the right hand terms can be distinguished only for the underlined distance-dependent linear phase shifts, which causes simple translations of the warped signals on the warped time axis. This property can be fruitfully exploited by using signal correlation techniques and Eq. (1), since in the frequency domain the cross-correlation of two warped signals $s_w = s_{w_i} \star s_{w_k}$ is:

$$
\begin{aligned}
\mathbf{F}\left\{s_w\right\} &= \mathbf{FW}_w\left\{s(t, D_i)\right\} \cdot (\mathbf{FW}_w)^*\left\{s(t, D_k)\right\} \\
&= \mathbf{F}_w\left\{s(t, D_i)\right\} \cdot (\mathbf{F}_w)^*\left\{s(t, D_k)\right\} \\
&= \dot{w}(f) \cdot |S_0(w(f), 0)|^2 \cdot e^{-j2\pi fK(D_i - D_k)}
\end{aligned}
$$

Thus, the abscissa value at which the cross-correlation envelope of two signals peaks in the warped domain can be directly related to the difference in distance of propagation by the two dispersive signals. The algorithm graph is shown in Fig. 4.
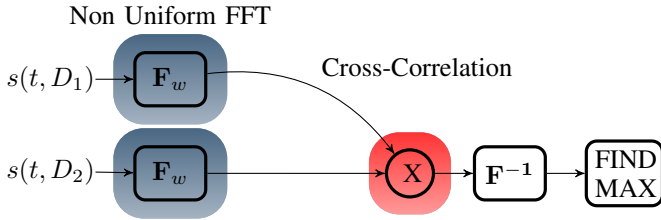

Fig. 4. Graph of the proposed localization algorithm

C. Hyperbolic positioning

Given the coordinates of the sensors positions (x_i, y_i) and having estimated the differences in traveled distance Δd_{1i} between the waves acquired by the first sensor and the remaining, a hyperbolic positioning method (also called $multilateration$) can be applied to locate the point source.

$$
\Delta d_{1i} = \sqrt{(x_1 - x_p)^2 + (y_1 - y_p)^2} - \sqrt{(x_i - x_p)^2 + (y_i - y_p)^2}
$$

The intersection of the different hyperbolas, obtained by solving the system of $M - 1$ equations (where M is the number of sensors) with the Levenberg-Marquardt algorithm [11], is taken to be the impact position.

III. HARDWARE DESIGN

The system is composed by 4 different elements: (A) piezoelectric sensors, (B) acquisition chain, (C) processing electronic unit and (D) wireless transmission module.

(A) Piezoelectric sensors: when an impact occurs on an elastic structure, a stress wave is created and it propagates across the structure, radially from the point of impact. The proposed system exploits at least 4 conventional piezoelectric transducers arranged in a geometrical fashion.

(B) Acquisition chain: PZT transducers are connected directly with the ADC ports of the STM32F4 board and each ADC channel is configured in dual mode with 250 kHz maximum sampling frequency since generally the spectral components of the Lamb waves lower rapidly above 60-100 kHz. The acquired values are stored in a DMA circular buffer; when the maximum value of the buffer exceeds the threshold value the trigger is sent and the Micro Controller Unit (MCU) performs the localization algorithm. The acquisition settings are shown in Table I:

TABLE I.   ACQUISITION AND ADC SETTINGS

Inputs	4 sensors	Sampling frequency f_s	250 kHz
Input Range	±2 V	Samples	2048
Acquisition period	8 ms	Sample resolution	12 bit

(C) Processing electronic unit: the center of the system is the processing core which contains function modules for data collection, processing and communication control. A Cortex-M4 based board is selected as main chip in the processing core. The MCU is specifically a STM32F4 evaluation board featuring a STM32F407VGT6 microcontroller with 1 MB Flash and 192 KB RAM. The strength point of the core is the CPU with FPU, adaptive real-time accelerator allowing 0-wait state execution from Flash memory and frequency up to 168 MHz. The computational cost of the proposed localization algorithm is shown in Table II.

TABLE II.   ALGORITHM COMPUTATIONAL COST

Non Uniform FFT	
1) FFT	$N = J \times M = 2^{12}$ points: complexity $O(N \log N)$
2) MIN-MAX	memory $w(f)$: $J \times M = 2^{12}$; complexity $O(JM)$
	samples 12 bit: memory: $2^{12} \times 12 \approx 49$ KByte
Cross-Correlation: 3 products with signals of length 2^{11}	
Inverse FFT : $M = 2^{11}$ points complexity $O(M \log M)$	

(D) Wireless transmission module: when the device is used to monitor the structural health of large structures, each node in the network monitors a specific portion of the structure surface, eventually reporting to a central location in case of detected damage. The wireless communication technology allows long distance data transmission without wiring, simplifying the difficulties in multi-device network monitoring. To be compliant with the low-power requirements the device presents a RF wireless module ZigBee/IEEE802.15.4 compliant, connected to the main board using an Serial Peripheral Interface (SPI).

IV. EXPERIMENTAL VERIFICATION

We exploited the proposed SHM system to locate impacts in an aluminum 1050A square plate 1 m × 1 m and 3 mm thick. Four PZT discs (PIC181, diameter 10 mm, thickness 1 mm) were placed asymmetrically at the corners of a square as depicted in the experimental setup in Fig. 5.
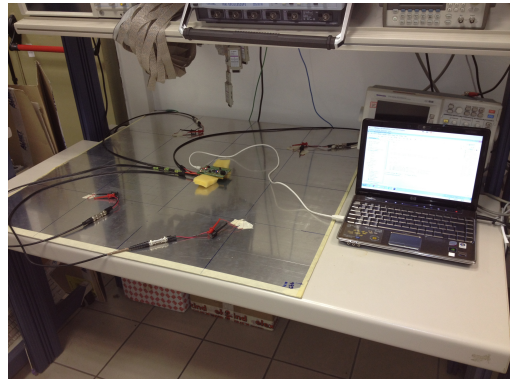

Fig. 5. Experimental setup

Guided waves were excited by pencil-lead breaks. The ADC channels of the STM32F4 discovery board were set in dual mode to continuously acquire signals with a maximum sampling frequency of 250 kHz. The board was supplied with 3.3 V. Data were recorded in a circular DMA buffer and

acquisitions triggered when the signal received from one of the PZT discs reached a threshold level of 50 mV. In order to analyse the dependency of the power consumption and the localization performances with the sampling frequency, experiments were carried changing the frequency in the range $[150 - 250]$ kHz. Results in Table III show how lowering the sampling frequency, the current consumption decreases but not in a linear manner; furthermore the MCU elaboration step is very sensible to the sampling frequency since the algorithm complexity is proportional to the sample buffer length which is reduced if the sampling frequency is lower.

TABLE III.   MEAN CURRENT CONSUMPTION

	ADC sampling	Signal Processing
$f_s = 250$ kHz	32 mA	63 mA
$f_s = 200$ kHz	27 mA	53 mA
$f_s = 150$ kHz	24 mA	50 mA

Fig. 6 shows the current consumption values measured for different sampling frequencies. Since the ADC sampling state is performed always in time the current reduction achieved with low frequency is noticeable. However, such reduction must be analysed with respect to the resolution achieved in the impact localization.
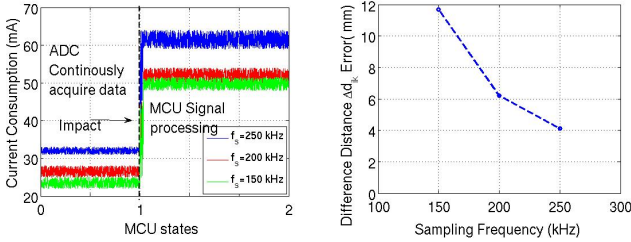

Fig. 6.   Current consumption for different sampling frequencies

Fig. 7.   Localization error for different sampling frequencies

In Fig. 7 is reported the mean error of the difference distance of arrival measured on a set of $K = 10$ of experimental impacts on the aluminum plate. The error is calculated as follow:

$$e = \frac{1}{3 * K} \sum_{k=1}^{K} \sum_{i=1}^{3} (\Delta d_{1i} - \Delta \hat{d}_{1i}) \quad k = 1, \ldots, 10;$$

As it can be seen from Fig. 7, lowering the sampling frequency the positioning error rises; in contexts such as wing monitoring, the high localization resolution is an important constrain because facilitates the decision to be taken in critical phases such as aircraft takeoff and optimizes the number of sensors to be used to monitor large areas.
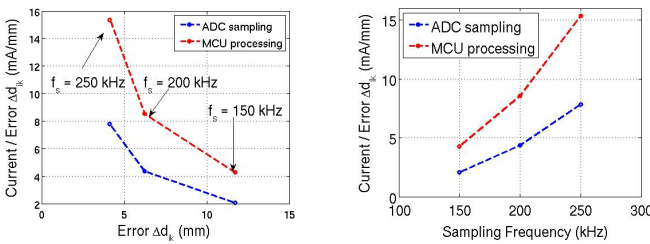

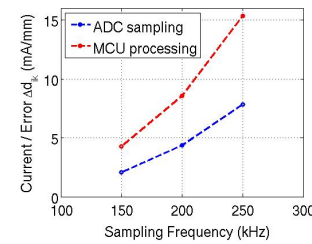Fig. 8.   Dependency of the localization error with the current

Fig. 9.   Dependency of $\frac{I_d\,(mA)}{e\,(mm)}$ with the sampling frequency

A good parameter able to take into account both the current consumption and the spatial resolution is $\frac{I_d\,(mA)}{e\,(mm)}$. Fig. 8 shows that $\frac{I_d\,(mA)}{e\,(mm)}$ is not constant, denoting that the impact localization error and the current consumption tends to be quadratic. Fig. 9 shows the dependency of $\frac{I_d\,(mA)}{e\,(mm)}$ with the sampling frequency.

V.   CONCLUSIONS

In this work an efficient wireless embedded structural monitoring system for impact localization based on Lamb waves is proposed. The method applies a dispersion compensation procedure on the signals acquired by passive sensors, thus overcoming the difficulties associated with arrival time detection based on classical thresholding procedures. The processing framework and the algorithm are implemented on a STM32F4 discovery board with advantages of compactness, low-power consumption, high efficiency and precision. The system was validated experimentally to locate impacts in a aluminum plate with four sparse PZT sensors. Results shows the effectiveness of the proposed implementation with high localization accuracy and low current consumption.

REFERENCES

[1] Perelli A., De Marchi L., Marzani A. and Speciale N. "Acoustic emission localization in plates with dispersion and reverberations using sparse PZT sensors in passive mode", Smart Mater. Struct. 21 (2012) 025010 (10pp).

[2] Boyle D., Magno M., O'Flynn B., Brunelli D., Popovici E. and Benini L., "Towards persistent structural health monitoring through sustainable wireless sensor networks", Intelligent Sensors, Sensor Networks and Information Processing (ISSNIP), 2011 Seventh International Conference on , pp.323-328, 6-9 Dec. 2011

[3] Benini L., Brunelli D., Petrioli C. and Silvestri S., "GENESI: Green sEnsor NEtworks for Structural monItoring", Sensor Mesh and Ad Hoc Communications and Networks (SECON), 2010 7th Annual IEEE Communications Society Conference on , pp.1-3, 21-25 June 2010

[4] Zhao X. *et al.*, "Active health monitoring of an aircraft wing with an embedded piezoelectric sensor/actuator network: II wireless approaches.", Smart Mater. Struct. 16 (2007) pp. 1218-1225.

[5] Liu L., and Yuan F.G., "Active damage localization for plate-like structures using wireless sensors and a distributed algorithm", Smart Mater. Struct. 17 (2008) 055022.

[6] Aygun B. and Gungor V.C., "Wireless sensor networks for structure health monitoring: recent advances and future research directions", Sensor Review, 31/3 (2011), pp. 261-276.

[7] Wilcox P. D., "A rapid signal processing technique to remove the effect of dispersion from guided wave signals", IEEE Trans. Ultrason. Ferroelectr., Freq. Control, 50 (2003), pp. 419-427.

[8] De Marchi L., Marzani A., Caporale S. and Speciale N., "Ultrasonic guided-waves characterization with warped frequency transforms", IEEE Trans.Ultrason. Ferroelectr. Freq. Control, 56 (2009), pp. 2232-2240.

[9] Bartoli I., Marzani A., Lanza di Scalea F. and Viola E., "Modeling wave propagation in damped waveguides of arbitrary cross-section", Journal of Sound and Vibration, 295 (2006), pp. 685-707.

[10] Fessler J., "Nonuniform fast Fourier transforms using min-max interpolation", IEEE Trans. Signal Processing, 51 (2003), pp. 560-574.

[11] Marquardt D., "An Algorithm for Least-Squares Estimation of Nonlinear Parameters", SIAM Journal on Applied Mathematics. 11 (1963).